2013 10th IEEE International Conference on Control and Automation (ICCA)
Hangzhou, China, June 12-14, 2013

Open Loop System Identification for a Quadrotor Helicopter System

R.J.A. Schreurs and S. Weiland Faculty of Electrical Engineering, Dept. of Control Systems
Eindhoven University of Technology
5612 AZ Eindhoven, The Netherlands
r.j.a.schreurs@student.tue.nl

H. Tao, Q. Zhang, J. Zhu*, Y. Zhu and C. Xu
Dept. of Control Engineering, Institute of Cyber-Systems and Control
Zhejiang University
310027, Hangzhou, Zhejiang, P.R. China
cxu@zju.edu.cn

***Abstract*— This paper explains how the method of system identification can be applied to a quadrotor helicopter. First the first principles model is studied. The open-loop model is an unstable system, which is simulated using a closed-loop scheme. Then, a 12th order Auto Regressive Moving Average with eXogenous inputs (ARMAX) model is obtained based on the simulation data.**

I. INTRODUCTION

A. General on UAVs

Unmanned Aerial Vehicles (UAVs), e.g. airplanes and drone helicopters are becoming increasingly popular, because they can be built in a wide range of sizes and can be controlled remotely from a distance. They form a basic aircraft that can be easily augmented with different sensing units for various applications such as unmanned reconnaissance flights, air photography, air filming or tracking or following of objects.

B. Related work

In the recent years several kinds of methods have been used for controlling quadcopters. Quadrotor system models are obtained using first principles modelling or the Prediction Error Minimization (PEM) system identification method. The testsignals for the PEM method are often generated manually during flight. Used control methods are e.g. classic (e.g. PD), Linear Quadratic Gaussian or Sliding Mode Control. Performance and stability are strongly dependent on the quality of the model and the choice of control method.
This paper applies the PEM system identification method using Generalized Binary Noise (GBN) signals as testsignals to identify a model with outputs height, roll, pitch and yaw. GBN signals are used to design a consistent identification method.

C. The quadrotor helicopter system

The quadrotor helicopter (or quadcopter in short) is a type of UAV that has four rotors in a square (see figure 1, making it possible to hover, move forward, sidewards, up, down, and turn about the roll, pitch and yaw axes separately. This makes the aircraft versatile and an approriate choice for many applications.
A description of the real quadcopter:

- Quadcopter frame: The quadcopter consists of a central body with 4 arms mounted in a star-wise configuration. A rotor is mounted at the end of each arm.
- Motors: Each rotor consist of a motor and a propeller and each motor is controlled by an Electronic Speed Controller (ESC). The input of an ESC is a Pulse Width Modulated (PWM) input signal. The dutycyles of all PWM signals are measured for the purpose of system identification.
- Sensors: There are four sensors mounted on the quadcopter for measurements. An Inertial Measurement Unit (IMU) is used to measure vertical acceleration, roll, pitch and yaw. An ultrasonic distance sensor is used for measuring height.
- Microcontroller Unit (MCU): An MCU is mounted on the central body and is connected to the sensors and the motor controllers. The MCU is used to implement the controller that stabilizes and controls the quadcopter. The MCU also communicates wirelessly with a computer to receive reference signals and send measurement data.
- Wireless transceiver: A radio frequency (RF) transceiver is used for wireless communication between the quadcopter and the base computer.
- Computer: A computer will automatically conduct the experiments with the quadcopter.

The propellers on the quadcopter provide lift for the UAV. The rotational inertia of the propellers enables control of the complete attitude by varying the rotational speeds of the four motors individually.

D. Motivation for system identification

The identification method has several advantages:

1) When modelling is done by using first principle models, often several experiments have to be conducted to obtain all parameters of the model. Many of those parameters are hard to measure in an experiment. This costs a lot of work and does not guarantee accuracy, because important dynamics may not occur in the first principles model.
2) The method can be used as a general framework for modelling similar quadcopter systems. For example, using different sensing units, motors or propellers changes the dynamics.

*UCSD former student who contributed with the simulation

978-1-4673-4708-2/13/$31.00 ©2013 IEEE

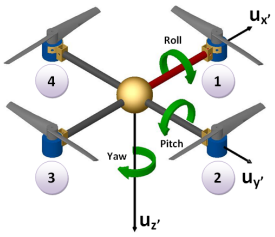

Fig. 1. A quadcopter with definition of height, roll, pitch and yaw

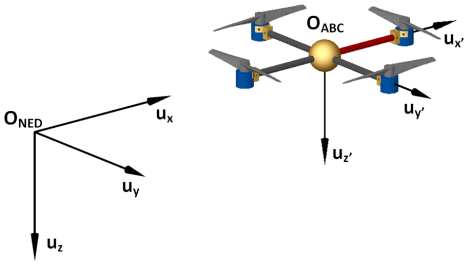

Fig. 2. Frames of reference: $\mathcal{O}_{NED}$ (left) and $\mathcal{O}_{ABC}$ (right)

3) The method has the potential to synthesize advanced controllers in an embedded chip (Control Module on Chip (CMC)).

II. Mathematical modeling based on first principle laws

A. Frames of reference

The quadcopter's dynamics are defined using two frames of reference: the earth fixed $\mathcal{O}_{NED}$ frame and the body fixed $\mathcal{O}_{ABC}$ frame, respectively. See figure 2.
$\mathcal{O}_{NED}$ is the frame fixed to the earth, in which u_x points North, u_y points East and u_z points Down. $\mathcal{O}_{ABC}$ is the frame fixed to the quadcopter's body, in which u'_x, u'_y and u'_z are defined along the axes of the quadcopter. The dynamical system of the quadcopter is defined by 12 state variables in total.

- 6 states define the position of the system in the 3-dimensional space: Cartesian coördinates (x,y,z) point at the center of gravity (COG) of the quadcopter in the $\mathcal{O}_{NED}$ frame. Their time derivatives (u,v,w) define the speed of the COG relative to the earth, defined in the $\mathcal{O}_{ABC}$ frame.
- Another 6 states define the attitude of the system: The Euler angles (ϕ,θ,ψ), representing roll, pitch and yaw respectively, are defined in the $\mathcal{O}_{NED}$ frame. Their time derivatives (p,q,r), defined in the $\mathcal{O}_{ABC}$ frame, describe the rotation of the quadcopter about its axes.

B. Dynamic model

The nonlinear first principle model is taken from equations (3.30) and (3.21) of "Modelling, Identification and Control of a Quadrotor Helicopter" [1]. A friction of the air with parameter k is added to the equation for $\ddot{z}$, so, this friction is not neglected. The model has system input $u=(\Omega_1,\Omega_2,\Omega_3,\Omega_4)$, of which Ω_i represents the rotational speed of the motor with number i. The model has system output $\xi=(\dot{x},\dot{y},\dot{z},p,q,r)^T$. Equation (1) describes the first principles model.

$$\xi=\begin{bmatrix}\dot{x}\\ \dot{y}\\ \dot{z}\\ p\\ q\\ r\end{bmatrix} \quad u=\begin{bmatrix}\Omega_1\\ \Omega_2\\ \Omega_3\\ \Omega_4\end{bmatrix} \quad \dot{\xi}=f(\xi,u) \tag{1}$$

This state space model is nonlinear and includes inertial moments (m,I_{xx},I_{yy},I_{zz}), the gyroscope effect (J_{TP}) and friction in the air (k).
In the simulation model, we use the following values for all parameters. These values are used in [1].

- $m=1$kg Total mass of the quadcopter
- $I_{xx}=8.1\cdot10^{-3}$kgm^2 Body moment of inertia around x-axis
- $I_{yy}=8.1\cdot10^{-3}$kgm^2 Body moment of inertia around y-axis
- $I_{zz}=14.2\cdot10^{-3}$kgm^2 Body moment of inertia around z-axis
- $J_{TP}=104\cdot10^{-6}$kgm^2 Rotational moment of inertia around a propeller axis
- $g=9.81$ms^{-2} Gravitational acceleration
- $l=0.24$m Length of COG to the center of the propeller
- $b=54.2\cdot10^{-6}$Ns^2 Thrust factor
- $d=1.1\cdot10^{-6}$kgm^2 Drag factor
- $k=0.5$s^{-1} Friction factor

C. Simplified model

The first principles model is nonlinear. The identification method estimates a linear model, which is a linear approximation of the nonlinear first principles model around the working point (ξ_0,u_0). A linearization of the system in equation (1) has the form:

$$\dot{\xi}=A(\xi-\xi_0)+B(u-u_0) \tag{2}$$

The working point (ξ_0,u_0) of the quadcopter is set to be $\xi_0=(0,0,0,0,0,0)^T$ and $u_0=(\Omega_{1_0},\Omega_{2_0},\Omega_{3_0},\Omega_{4_0})^T$. The values for Ω_{i_0} are defined such that $f(\xi_0,u_0)=0$.

In the working point, the system is level and therefore the $\mathcal{O}_{NED}$ frame and $\mathcal{O}_{ABC}$ frame are aligned, therefore all rotation factors can be considered constants. This leads to the assumptions in equations (3) to (6).

$$\left.\begin{aligned}\sin\psi_0\sin\phi_0 &= 0\\ \cos\psi_0\sin\theta_0\cos\phi_0 &= 0\end{aligned}\right\}\longrightarrow \ddot{x}\approx 0 \tag{3}$$

$$\left.\begin{aligned}-\cos\psi_0\sin\phi_0 &= 0\\ \sin\psi_0\sin\theta_0\cos\phi_0 &= 0\end{aligned}\right\}\longrightarrow \ddot{y}\approx 0 \tag{4}$$

$$\cos\theta_0\cos\phi_0=1\longrightarrow \ddot{z}\approx -g-k\dot{z}+\frac{U_1}{m} \tag{5}$$

$$T(\xi_0)=I\longrightarrow\begin{bmatrix}\dot{\phi}\\ \dot{\theta}\\ \dot{\psi}\end{bmatrix}\approx\begin{bmatrix}p\\ q\\ r\end{bmatrix} \tag{6}$$

Where U_1 represents the overall input from u to z and T describes the rotation between the $\mathcal{O}_{NED}$ and $\mathcal{O}_{ABC}$ frames.

In the linearized model, x and y are constant, therefore they will be omitted. Also, because the Electronic Speed Controllers have pulsewidth modulated (PWM) inputs, the inputs Ω_i in input vector u can be replaced with PWM_i.

In the rest of the paper, let u and $y = (\dot{z}, \dot{\phi}, \dot{\theta}, \dot{\psi})^T$ denote the input and output vectors of the linearized system, respectively. This results in the model in equation (7).

$$y = \begin{bmatrix} \dot{z} \\ \dot{\phi} \\ \dot{\theta} \\ \dot{\psi} \end{bmatrix}, \quad u = \begin{bmatrix} PWM_1 \\ PWM_2 \\ PWM_3 \\ PWM_4 \end{bmatrix}, \quad \dot{y} = A(y - y_0) + B(u - u_0) \quad (7)$$

This is a 4 input 4 output multi-input multi-output (MIMO) system. The outputvector y only contains derivatives, which means that the system from u to y has an integrator on all four outputs.

Together, these assumptions linearize all nonlinear parts of the nonlinear model, except for the coupling between the states p, q and r through the inertial moments. This coupling is quadratic in p, q and r and since those variables are small during the test, this coupling would probably be small too. However, because this coupling represents an important part in the dynamics of the quadcopter, it is not neglected. Otherwise, the nonlinear model may become oversimplified and may not provide enough insight for tuning the identification.

D. Controller

The controller used for acquiring measurement data is based on the reverse model or inverse dynamics, see equation (8).

$$\begin{bmatrix} PWM_1 \\ PWM_2 \\ PWM_3 \\ PWM_4 \end{bmatrix} = 1260 + 0.5\sqrt{M_{inv} \cdot C_{PID}(s)(r - y)} \quad (8)$$

$$M_{inv} = \begin{bmatrix} \frac{1}{4bl} & 0 & -\frac{1}{2bl} & -\frac{1}{4d} \\ \frac{1}{4bl} & -\frac{1}{2bl} & 0 & \frac{1}{4d} \\ \frac{1}{4bl} & 0 & \frac{1}{2bl} & -\frac{1}{4d} \\ \frac{1}{4bl} & \frac{1}{2bl} & 0 & \frac{1}{4d} \end{bmatrix} \quad (9)$$

$$C_{PID}(s) = \begin{bmatrix} \frac{m}{cos\phi\, cos\theta}\left(0.5\frac{s+0.002}{s} + g\right) & 0 & 0 & 0 \\ 0 & 1 & 0 & 0 \\ 0 & 0 & 1 & 0 \\ 0 & 0 & 0 & 1 \end{bmatrix} \quad (10)$$

Signal r in equation (8) represents the setpoint in the closed loop configuration. Figure 3 shows the step response of the closed loop system. It shows second order underdamped behaviour for all four outputs. The natural frequency is $f_n \approx 0.15Hz$, $t_{peak} \approx 3s$ and $t_{settling} \approx 20s$. A sampling time of 80ms is chosen, because it is the fastest sample rate that can be achieved by the hardware while conducting the experiments.

III. Open Loop Identification

A. Theory framework

The Prediction Error Method (PEM) is used for system identification. The real, data generating system can be described like in equation (11). $G(q)$ is the real system and $H(q)$ is the noise model. The signal $e(t)$ is assumed to be a white noise,

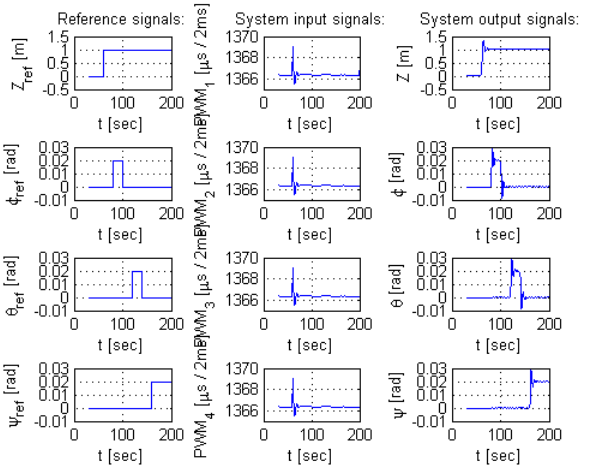

Fig. 3. Response of z, ϕ, θ, ψ to step inputs on r in closed loop

$$y(t) = G(q)u(t) + v(t) \quad (11)$$
$$= G(q)u(t) + H(q)e(t). \quad (12)$$

Let the generated data or observations, be denoted by $Z^N = \{(u(t), y(t)) | t = 1, ..., N\}$ and let the proposed identified model be denoted by $\hat{G}(q, \theta)$, the identified noise model by $\hat{H}(q, \theta)$ and the set of model parameters by θ. The identified system can be described by equation (13),

$$\hat{y}(t) = \hat{G}(q, \hat{\theta})u(t) + v(t) \quad (13)$$
$$= \hat{G}(q, \hat{\theta})u(t) + \hat{H}(q, \hat{\theta})e(t) \quad (14)$$

Using the observations and an identified model, the error signal $e(t)$ can be predicted, called the prediction error (equation (15) ,

$$\varepsilon(t) := y(t) - \hat{y}(t|t-1) = \hat{H}^{-1}(q)\left[y(t) - \hat{G}(q)u(t)\right] \quad (15)$$

The prediction error structure is shown in figure 4.

Now, the set of parameters $\hat{\theta}_N$ that minimizes the prediction error $\varepsilon(t)$ is defined by equation (16).

$$\hat{\theta}_N = arg\min_{\theta} \frac{1}{N}\sum_{t=1}^{N} \varepsilon^2(t, \theta) \quad (16)$$

The possible choices for model structures of $\hat{G}(q, \theta)$ are ARX (Auto Regressive eXogenous input), ARMAX, OE (Output Error) and BJ (Box-Jenkins).

$$\text{ARX}: \hat{G}(q, \theta) = \frac{B(q, \theta)}{A(q, \theta)}, \qquad \hat{H}(q, \theta) = \frac{1}{A(q, \theta)} \quad (17)$$

$$\text{ARMAX}: \hat{G}(q, \theta) = \frac{B(q, \theta)}{A(q, \theta)}, \qquad \hat{H}(q, \theta) = \frac{C(q, \theta)}{A(q, \theta)} \quad (18)$$

$$\text{OE}: \hat{G}(q, \theta) = \frac{B(q, \theta)}{F(q, \theta)}, \qquad \hat{H}(q, \theta) = 1 \quad (19)$$

$$\text{BJ}: \hat{G}(q, \theta) = \frac{B(q, \theta)}{F(q, \theta)}, \qquad \hat{H}(q, \theta) = \frac{C(q, \theta)}{D(q, \theta)} \quad (20)$$

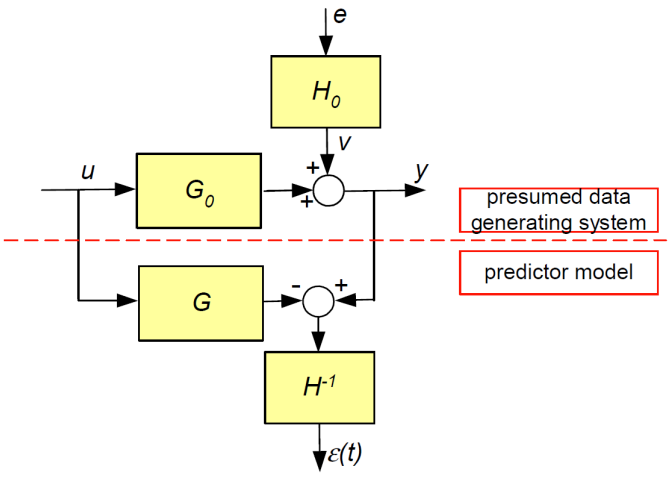

Fig. 4. Prediction Error model structure (from Van den Hoff [12])

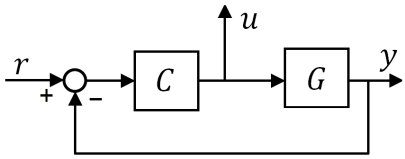

Fig. 5. Closed loop configuration. u and y are used as observation data

The orders of the polynomials in q, which are A, B, C, D and F, are denoted n_a, n_b, n_c, n_d and n_f respectively. An additional order n_k is specified to represent delays in the model.

B. Simulation environment

The first principle model is built in MATLAB Simulink and used for generating the observations Z^N. Because the system has integrators, it is unstable and therefore the observation data can only be acquired by conducting a test in a closed loop configuration, as shown in figure 5. The testsignal will be applied to the closed loop input r, which represents the setpoints for z, ϕ, θ and ψ.
The input signals PWM_i (here: u) and output signals y of the plant from the closed loop test are used for an identification of the plant itself (open loop).
The validation of the model was also performed using the same Simulink model, but with the first principle model replaced by the identified model.

C. Test signal design

The test signal is a Generalized Binary Noise (GBN) signal. Because a GBN signal has zero mean, limited bandwidth, continuous power spectrum and excites the system persistently of any order.

A GBN signal takes two amplitudes: $-\alpha$ and α. The rule in equation (21) determines the switching behaviour at each switching time.

$$\begin{aligned} P[u(t) = -u(t-1)] &= p_{sw} \\ P[u(t) = u(t-1)] &= 1 - p_{sw} \end{aligned} \tag{21}$$

The switching probability is 0.5. The minimum switching time T_{min} defines the minimum time for the signal to remain constant. This leads to an average switching time of $ET_{sw} = \frac{T_{min}}{p_{sw}}$. The average switching time can be changed to tune the bandwidth of the test signal.

- The amplitudes of the test signals are $\alpha_z = 0.02\text{m}, \alpha_\phi = 0.02\text{rad} (\approx 1\,\text{deg}), \alpha_\theta = 0.02\text{rad}, \alpha_\psi = 0.02\text{rad}$. These values are small enough for the quadcopter to behave linearly and large enough to be measured.
- T_{min} was chosen to be $80ms$.
- The average switching time is chosen at $ET_{sw} = 800\text{ms}$. This is about 3.75 times the peak time $t_{peak} = 3\text{s}$, so that the bandwidth of the testsignals is high enough.
- The duration is chosen to be 10 times the settling time $t_{settling} \approx 20\text{s}$. That gives $duration = 200\text{s}$, which is equivalent to $N = \frac{duration}{T_s} = \frac{200\text{s}}{80\text{ms}} = 2500$ samples.

The experiment is repeated once to obtain two separate sets of observations. The estimation set is used to estimate the model and the validation set is used to validate the model.

D. Model structure

The ARMAX structure is chosen, because it is numerically stable and unbiased. The other model structures have disadvantages: ARX is biased, while OE has no noise model and only white noise disturbances are modelled. The optimization algorithm for BJ is unstable when identifying an unstable model.

E. Order selection

The first principle model of the quadcopter has integrators on all outputs. Integrators are numerically unstable and cannot be identified. Therefore, the transfer function matrix from inputs (U_1, U_2, U_3, U_4) to the output *derivatives* $(\dot{z}, p, q, r)$ is measured. This is a first order model.
Another way of selecting the order is using the estimation data based Final Prediction Error (FPE) in equation (22) as a measure of accuracy of the model fit.

$$V_{PE}^E = \sum_{t=1}^{N} H^{-1}(q)\,[\dot{y}(t) - G(q)u(t)]^2 \tag{22}$$

Figure 6 shows that the order must be at least 1. From practice it followed that, given this testsignal, order 2 gives a more accurate fit, because of nonlinearity in the model.

The selected orders for the ARMAX structure are given by equations (23) and (24),

$$n_a = 2, \quad n_b = \begin{bmatrix} 2 & 2 & 2 & 2 \\ 0 & 2 & 0 & 2 \\ 2 & 0 & 2 & 0 \\ 2 & 2 & 2 & 2 \end{bmatrix} \tag{23}$$

$$n_c = \begin{bmatrix} 2 \\ 2 \\ 2 \\ 2 \end{bmatrix}, \quad n_k = \begin{bmatrix} 0 & 0 & 0 & 0 \\ 0 & 0 & 0 & 0 \\ 0 & 0 & 0 & 0 \\ 0 & 0 & 0 & 0 \end{bmatrix} \tag{24}$$

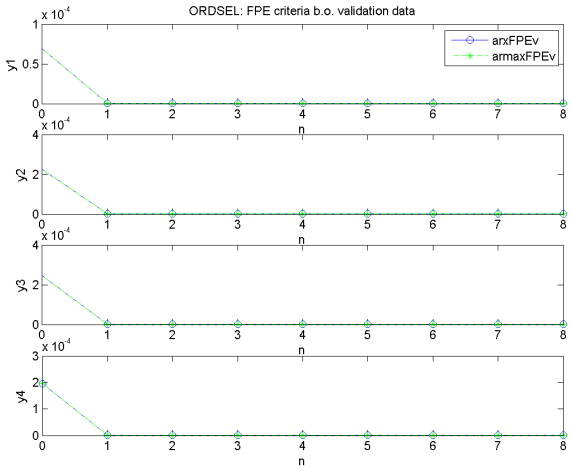

Fig. 6. FPE order selection

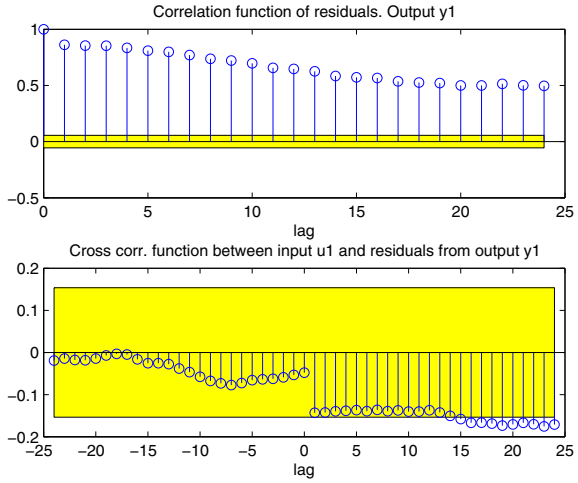

Fig. 7. Residual tests on output z of identified models.

F. Identification based on simulation

The identification has been tested on the first principle model from section (II-B). An identification is performed in MATLAB using the `model = armax(data, orders)` function:

```
MdlARMAX1 = armax(estdata1, [na nb1 nk1]);
MdlARMAX2 = armax(estdata2, [na nb2 nk2]);
MdlARMAX3 = armax(estdata3, [na nb3 nk3]);
MdlARMAX4 = armax(estdata4, [na nb4 nk4]);
```

IV. Results

The state space matrices A, B, C and D of the identified ARMAX model, denoted by $\hat{G}(q,\hat{\theta})$, are given by equation (25) to (28):

$$A = \begin{bmatrix}
1 & 0 & 0.031 & 0 & 0 & 0 & 0 & 0 & 0 & 0 & 0 & 0 \\
0 & 0 & -0.45 & 0 & 0 & 0 & 0 & 0 & 0 & 0 & 0 & 0 \\
0 & 0.5 & 1.2 & 0 & 0 & 0 & 0 & 0 & 0 & 0 & 0 & 0 \\
0 & 0 & 0 & 1 & 0 & 0.13 & 0 & 0 & 0 & 0 & 0 & 0 \\
0 & 0 & 0 & 0 & 0 & 0.19 & 0 & 0 & 0 & 0 & 0 & 0 \\
0 & 0 & 0 & 0 & 0.13 & 0.94 & 0 & 0 & 0 & 0 & 0 & 0 \\
0 & 0 & 0 & 0 & 0 & 0 & 1 & 0 & 0.13 & 0 & 0 & 0 \\
0 & 0 & 0 & 0 & 0 & 0 & 0 & 0 & 0.19 & 0 & 0 & 0 \\
0 & 0 & 0 & 0 & 0 & 0 & 0 & 0.13 & 0.94 & 0 & 0 & 0 \\
0 & 0 & 0 & 0 & 0 & 0 & 0 & 0 & 0 & 1 & 0 & 0.031 \\
0 & 0 & 0 & 0 & 0 & 0 & 0 & 0 & 0 & 0 & 0 & 0.25 \\
0 & 0 & 0 & 0 & 0 & 0 & 0 & 0 & 0 & 0 & 0.13 & 0.93
\end{bmatrix} \tag{25}$$

$$B = \begin{bmatrix}
9.8e-05 & 9.7e-05 & 9.1e-05 & 9.4e-05 \\
-0.0014 & -0.0014 & -0.0013 & -0.0013 \\
0.023 & 0.022 & 0.022 & 0.022 \\
0 & -0.013 & 0 & 0.013 \\
0 & -0.019 & 0 & 0.019 \\
0 & -0.21 & 0 & 0.21 \\
-0.013 & 0 & 0.013 & 0 \\
-0.02 & 0 & 0.02 & 0 \\
-0.21 & 0 & 0.21 & 0 \\
-0.00059 & 0.0005 & -0.00064 & 0.00072 \\
-0.0047 & 0.004 & -0.005 & 0.0057 \\
-0.041 & 0.041 & -0.041 & 0.042
\end{bmatrix} \tag{26}$$

$$C = \begin{bmatrix}
0.32 & 0 & 0 & 0 & 0 & 0 & 0 & 0 & 0 & 0 & 0 & 0 \\
0 & 0 & 0 & 0.32 & 0 & 0 & 0 & 0 & 0 & 0 & 0 & 0 \\
0 & 0 & 0 & 0 & 0 & 0 & 0.32 & 0 & 0 & 0 & 0 & 0 \\
0 & 0 & 0 & 0 & 0 & 0 & 0 & 0 & 0 & 0.32 & 0 & 0
\end{bmatrix} \tag{27}$$

$$D = \begin{bmatrix}
0 & 0 & 0 & 0 \\
0 & -0 & 0 & 0 \\
-0 & 0 & 0 & 0 \\
-0 & 0 & -0 & 0
\end{bmatrix} \tag{28}$$

The identified model is validated by using two methods:

1) By conducting a residual test, the error residual test calculates the error given the identified plant model $\hat{G}$ and noise model $\hat{H}$ and validation data. The autocorrelation of the error must approximate the autocorrelation of a white noise, so it must approximate a dirac-pulse. The crosscorrelation must be zero for negative lag for the system to represent a causal system.
2) By placing it in closed loop with the controller in equation (21) and comparing the response to the same reference trajectory as shown in figure 3. The responses of both models are very similar. The natural frequency and damping is almost the same.

Figures 7 and 8 show the worst results of the residual test. Only the correlations of input PWM_1 to z and θ are shown, because these are not validated. The models for ϕ and ψ are very accurate.

The following can be concluded based on the residual test:

- The model for output z, shown in figure 7, shows that this model is not validated. The autocorrelation function is not a dirac pulse. Causality is confirmed, since it is well within the 99% bounds for negative lag.
- The model for output θ, shown in figure 8 is almost validated. The autocorrelation reaches just outside the 99% bound. However, this model can be considered to be useful.

Figure 9 and 10 show the closed loop simulations of not yet validated identified models of all four structures (ARX, ARMAX, OE and BJ).

The ARX and ARMAX models in figure 9 show a very good accuracy. The damping and settling times are almost the same as for the original system. The overshoot is slightly larger for both ARX and ARMAX. The ARMAX model has a smaller steady state error compared to the ARX model. Both models have almost no coupling between the outputs (response at $t = 160$s).

The OE and BJ models in figure 10 obviously perform worse. The OE model shows a bad low frequent behavior, which results in a large error that takes minutes to reduce to a small value. Furthermore, there is much more coupling between the outputs of the OE and BJ models, while there is almost none for the original model. This shows that the OE and BJ

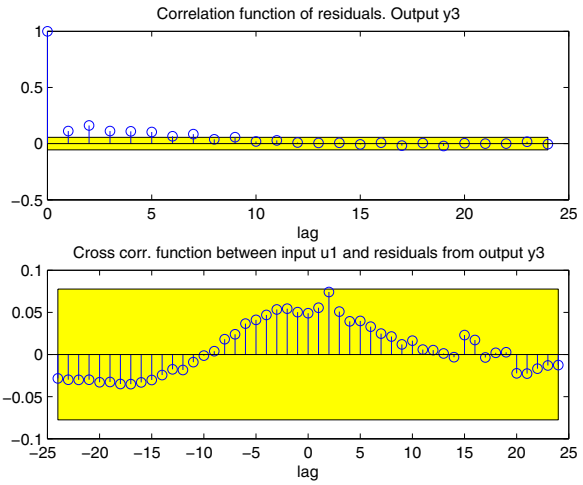

Fig. 8. Residual tests on output θ of identified models.

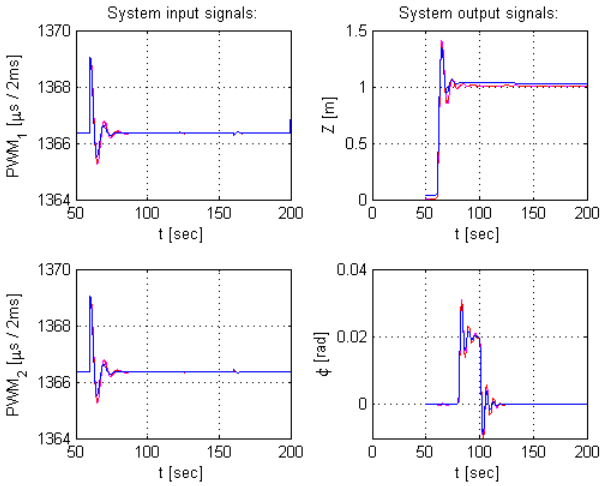

Fig. 9. Trajectory responses of original (blue, solid) and identified model (ARMAX: red, dashed, ARX: magenta, solid)

models cannot be validated.

V. Conclusion & Future Research

The quadcopter system can be identified accurately by identifying the differentiated model with a second order ARMAX structure and adding the integrators manually.

Further research can be aimed at improving the quality of the identified model by using different duration of the test, amplitude or bandwidth of the testsignal or higher sample rate.

Furthermore, the method can be applied to practice and improved for an implementation in e.g. automated identification systems in a Control Module on Chip.

The MIMO model identified by using the method in this paper, can be used for designing a MIMO controller.

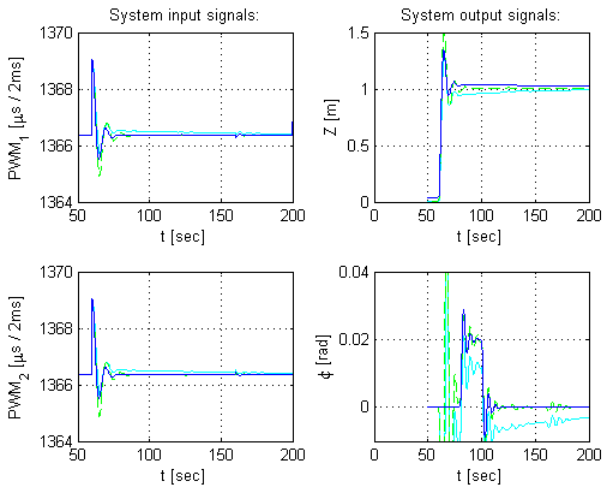

Fig. 10. Trajectory responses of original (blue, solid) and identified models (OE: cyan, solid and BJ: green, dashed)

It is suitable for Robust Control, because the identification algorithm in MATLAB also calculates a covariance matrix corresponding to the model parameters. This covariance matrix can be used for defining an upper and lower bound on the parameters.

References

[1] T. Bresciani, Modelling, Identification and Control of a Quadrotor Helicopter A Master's thesis of the Department of Automatic Control, Lund University, Lund, Sweden, 2008.

[2] J. M. B. Domingues, Quadrotor prototype Universidade Técnica de Lisboa, Lisbon, Portugal, 2009.

[3] G. Lee, D. Y. Jeong, N. D. Khoi, T. Kang, Attitude Control System Design for a Quadrotor Flying Robot, The 8th International Conference on Ubiquitous Robots and Ambient Intelligence (URAI), 2011, p.74-78.

[4] D. Lee, H. Kim, S. Sastry, Feedback Lineariztion vs. Adaptive Sliding Mode Control for a Quadrotor Helicopter, International Journal of Control, Automation and Systems, 2009, p.419-428.

[5] P. Pounds, R. Mahony, P. Corke, Modelling and Control of a Quad-Rotor Robot, Australian National University, Canberra, CSIRO ICT Centre, Brisbane, Australia.

[6] Derek Scott Miller, Open Loop System Identification of a Micro Quadrotor Helicopter from Closed Loop Data, A Master's thesis of the Department of Aerospace Engineering of the University of Maryland, 2011.

[7] H. Bouadi, M. Bouchoucha, M. Tadjine, Sliding Mode Control based on Backstepping Approach for an UAV Type-Quadrotor, World Academy of Science, Engineering and Technology 26, 2007, p.22-27.

[8] G. Lee, D. Y. Jeong, N. D. Khoi, T. Kang, Attitude Control System Design for a Quadrotor Flying Robot, The 8th International Conference on Ubiquitous Robots and Ambient Intelligence (URAI), 2011, p.74-78.

[9] I. Sa, P. Corke, System Identification, Estimation and Control for a Cost Effective Open-Source Quadcopter, IEEE International Conference on Robotics and Automation, RiverCentre, Saint Paul, Minnesota, USA, May 14-18, 2012, p.2203-2209.

[10] Y. Bai, H. Liu, Z. Shi, Y. Zhong, Robust Control of Quadrotor Unmanned Air Vehicles, Proceedings of the 31st Chinese Control Conference July 25-27, Hefei, China, 2012, p.4462-4467.

[11] Y. Zhu, Multivariable System Identification for Process Control Eindhoven University of Technology, Eindhoven, The Netherlands, 2011.

[12] P. v. d. Hoff, System Identification, Data-Driven Modeling of Dynamic Systems. Lecture Slides, Eindhoven University of Technology, Eindhoven, The Netherlands, 2012.